Numerical Analysis of Leaky Lamb Wave Propagation Using a Semi-Analytical Finite Element Method

Takahiro Hayashi[1, a)] and Daisuke Inoue[1]

[1]*Kyoto University*
Kyotodaigaku-katsura C3 bld., Nishikyo-ku, Kyoto 615-8540, Japan

[a)]Corresponding author: hayashi@kuaero.kyoto-u.ac.jp

Abstract. Dispersion curves and wave structures for leaky Lamb waves were numerically analyzed with a semi-analytical finite element method. Solving governing equations derived for a leaky plate mode and a total transmission mode provided dispersion curves of fundamental Lamb modes and Scholte waves with several differences. The Scholte waves in the non-dispersive region were modes with large vibration in the vicinity of a single interface between a plate surface and fluid. Moreover, in low frequency-thickness product (*fd*) range in the dispersion curves, the Scholte waves became highly dispersive modes. Wave structures obtained for the Scholte wave in the SAFE calculations implied that the high dispersion in the low *fd* range is caused by the fact that wave energy of Scholte wave penetrates deeper in the plate in lower *fd* range and that the the opposite boundary of the plate affects the Scholte wave.

INTRODUCTION

A semi-analytical finite element (SAFE) method has been widely used as one of the most suitable calculation technique for guided wave propagation because the calculation technique that does not require descretizing the propagation direction enables us to carry out very efficient calculation and modal analysis even for large plate-like structures. The SAFE in a broad sense was firstly developed by Cheung [1] for analyzing static deformation of civil engineering structures, and then Dong and Nelson [2], Datta et al. [3], and Kausel et al. [4] extended it to dynamic problems, e. g. Lamb waves in a laminated plate. For noise analysis of a railway rail, Gavric [5], Gry [6], Thompson and Jones [7] derived dispersion curves for a rail with a SAFE. Recently, Loveday [8], Castaings and Lowe [9], Mazzotti et al. [10] and authors [11] have developed and performed SAFE calculations for the purpose of guided wave nondestructive evaluation.

However, most of the SAFE calculations were developed on the assumption of stress free boundaries without considering leakage to external media, and very few papers [9, 12] considered such leakage to external air, water and soil that sometimes significantly affect actual guided wave nondestructive evaluation.

Authors then formulated a SAFE for a plate with external fluids using the characteristic that plane harmonic wave propagates in the fluids for a certain mode and at a certain frequency [13]. This paper briefly describes the formulation by comparing with one without external media, and then discusses fundamental modes and Scholte waves obtained by the SAFE technique.

A SEMI-ANALYTICAL FINITE ELEMENT METHOD FOR LEAKY LAMB WAVE

When considering a plate with no leaky media and with stress-free boundaries as shown in Fig. 1 (a), a governing equation is obtained in angular frequency ω domain and wave number ξ_z domain as,

$$\left(\mathbf{K}_1 + \xi_z \mathbf{K}_2 + \xi_z{}^2 \mathbf{K}_3 - \omega^2 \mathbf{M}\right)\mathbf{U} = 0\,, \tag{1}$$

where, letting N be the number of nodal lines in a plate with layered elements, $\mathbf{K}_1$, $\mathbf{K}_2$, $\mathbf{K}_3$, and $\mathbf{M}$ are $2N$ x $2N$ matrices obtained from known geometric and material parameters such as thickness of layered elements and material properties, and $\mathbf{U}$ is a $2N$ vector consisting of nodal displacements. Suppose that angular frequency ω is fixed, eq. (1) can be regarded as the second order polynomial eigenvalue problem with respect to ξ_z. Then it can be generally developed into the following linear eigenvalue problem with $4N$x4N matrices **A** and **B**.

$$\left(\mathbf{A}-\xi_z\mathbf{B}\right)\begin{pmatrix}\mathbf{U}\\ \xi_z\mathbf{U}\end{pmatrix}=0\,, \tag{2}$$

where

$$\mathbf{A}=\begin{pmatrix}\mathbf{0} & \mathbf{I}\\ \mathbf{K}_1-\omega^2\mathbf{M} & i\mathbf{K}_2\end{pmatrix},\ \mathbf{B}=\begin{pmatrix}\mathbf{I} & 0\\ 0 & -\mathbf{K}_3\end{pmatrix}. \tag{3}$$

Solving $\det\left(\mathbf{A}-\xi_z\mathbf{B}\right)=0$, a necessary and sufficient condition for nontrivial solutions of eq. (2), provides $4N$ eigenvalues ξ_{zm} (m=1, 2,..., $4N$). The eigenvalues represent wavenumbers of possible resonant modes for harmonic wave with the angular frequency of ω, and are classified into two types; $2N$ modes in the +z direction and $2N$ modes in the -z direction.

On the other hand, when considering a plate surrounded by fluids with the same velocity (c_f) and different densities (ρ_1, ρ_2), the term of pressure from external fluids $\mathbf{F}$ is added to eq. (1) as,

$$\left(\mathbf{K}_1+\xi_z\mathbf{K}_2+{\xi_z}^2\mathbf{K}_3-\omega^2\mathbf{M}\right)\mathbf{U}=\mathbf{F} \tag{4}$$

Since the term of external pressure **F** depends only on displacements in the y direction at plate surfaces, the following relationship is established between **F** and **U**.

$$\mathbf{F}=\frac{\omega^2}{\xi_y}\mathbf{Q}\,\mathbf{U}, \tag{5}$$

As **F** is comprised of zero except y components at both upper and lower surfaces and the non-zero values depends only on a displacement in the y direction at the surfaces, **Q** is a $2N$ x $2N$ matrix having non-zero values only at two components. For example, when **F** and **U** are assigned in the order of y and z components at the node 1, y and z components at node 2,...., **Q** is written as,

$$\mathbf{Q}=\begin{pmatrix} i\rho_1 & 0 & \cdots & 0 & 0\\ 0 & 0 & & & 0\\ \vdots & & \ddots & & \vdots\\ 0 & & & i\rho_2 & 0\\ 0 & 0 & \cdots & 0 & 0\end{pmatrix},\qquad \mathbf{Q}=\begin{pmatrix} -i\rho_1 & 0 & \cdots & 0 & 0\\ 0 & 0 & & & 0\\ \vdots & & \ddots & & \vdots\\ 0 & & & i\rho_2 & 0\\ 0 & 0 & \cdots & 0 & 0\end{pmatrix}, \tag{6}$$

where the first equation is obtained when positive ξ_y is taken in the plus and minus directions in the upper and lower fluids respectively, representing modes radiating from the plate to the external fluids. While, the second equation in eq. (6) is obtained when positive ξ_y is taken in the plus direction in both upper and lower fluids, showing modes propagating through the plate. These modes, being obtained theoretically by Chimenti and Rocklin [14], are called leaky plate mode and total transmission mode, respectively.

Substituting eq. (5) into eq. (4) gives

$$\left(\mathbf{K}_1+\xi_z\mathbf{K}_2+{\xi_z}^2\mathbf{K}_3-\omega^2\mathbf{M}-\frac{\omega^2}{\xi_y}\mathbf{Q}\right)\mathbf{U}=0\,. \tag{7}$$

Because a plane harmonic wave propagates in fluids with the wavenumber of ξ_f (= ω/c_f), the following equation hold between ξ_y and ξ_z,

$${\xi_y}^2+{\xi_z}^2={\xi_f}^2\,. \tag{8}$$

In addition, a pair of possible resonance modes in plus and minus *z* directions always exists due to the symmetry of a plate. Using the relationship of eq. (8) and the symmetry of possible modes, the nonlinear eigenvalue problem eq. (7) can be converted into a linear eigenvalue problem with respect to ξ_y as,

$$\left(\mathbf{A}' - \xi_y \mathbf{B}'\right)\mathbf{U}' = 0\,, \tag{9}$$

where $\mathbf{A}'$, $\mathbf{B}'$ are known (4*N*+2) x (4*N*+2) matrices, and $\mathbf{U}'$ is a 4*N*+2 vector comprised of the nodal displacement vector $\mathbf{U}$ and wavenumber ξ_z. Solving the linear eigenvalue problem gives 4*N*+2 eigenvalues for ξ_y, and then eq. (8) provides 4*N*+2 pairs of $\pm\xi_z$, which represents the symmetry of resonance modes in the ±*z* directions. Moreover, eigenvectors obtained from eq. (9) provides cross-sectional displacement distributions (wave structures).

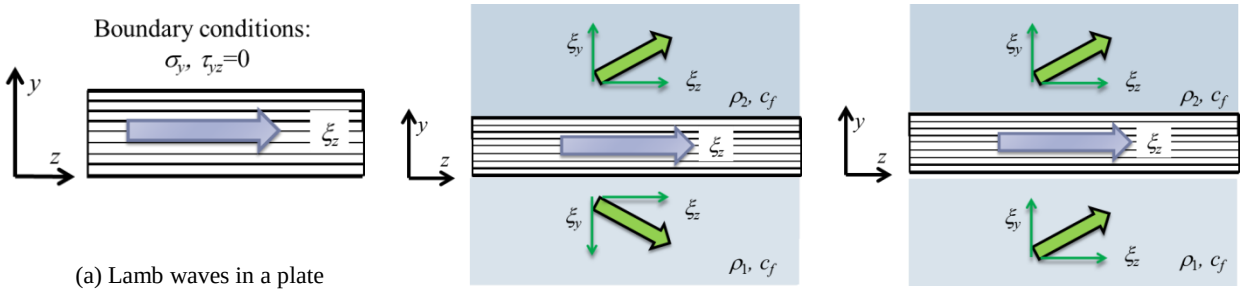

(a) Lamb waves in a plate with traction free boundaries

(b) Leaky plate mode

(c) Total transmission mode

FIGURE 1. Geometrical conditions for SAFE calculations.

CALCULATION RESULTS ON DISPERSION CURVES AND WAVE STRUCTURES

For a plate with no leaky media, eigenvalues of eq. (2) become wavenumbers of Lamb wave modes. Frequency spectra of the wavenumber, called dispersion curves, are widely used because they indicate fundamental characteristics of Lamb waves. For a plate with leaky media, eq. (9) and (8) provide wavenumbers in the *y* and *z* directions ξ_{ym} and $\pm\xi_{zm}$ (*m*=1, 2, ..., 4*N*+2).

In this section, we discuss dispersion curves and wave structures for an aluminum alloy plate (density of 2700kg/m^3, longitudinal and transverse velocities of 6400m/s and 3100m/s) surrounded by water (density of 1000kg/m^3 and sound velocity of 1500m/s) as a typical example of leaky Lamb waves.

Dispersion Curves and Wave Structures of Leaky Plate Modes

Figure 2 shows dispersion curves for leaky plate modes obtained from the first equation of eq. (6) in the representation of phase velocity ($c_{pm} = \omega/\xi_z$), group velocity ($c_{gm} = \partial\omega/\partial\xi_z$), and attenuation ($\mathrm{Im}(\xi_z)$). The only four lowest order modes with $\mathrm{Re}(\xi_{zm}) > 0$ or $\mathrm{Re}(\xi_{ym}) = 0$ and $\mathrm{Im}(\xi_{ym}) > 0$, corresponding to modes heading in the +*z* direction, are plotted. Horizontal axis stands for frequency - thickness product (*fd*).

We can find some differences from dispersion curves for a plate with no leaky media, which include the fact that: (i) non-dispersive modes with almost identical velocity to sound velocity of external fluids, called Scholte wave, exist, (ii) A0 and S0 modes attenuate due to energy leakage to fluids, and (iii) the curve of A0 mode is not smooth in the low *fd* range.

Figures 3, 4, and 5 show wave structures at the point A, B, and C on phase velocity dispersion curves in Fig. 2 (a). The wave structures denote displacement distributions at a certain moment in the 5*d* x 5*d* cross-sectional region including the plate of thickness *d* and fluids, and the surface color presents displacement in the *y* direction. As shown in Figs. 3 - 5, two different wave structures exist at A, B, and C on phase velocity dispersion curves, respectively. In the case of Fig. 3 where S0 mode propagates from left to right, outgoing and incoming modes are obtained where plane harmonic waves propagate outward to and inward from external fluids depending on the sign of $\mathrm{Re}(\xi_{ym})$. Energy leakage to external fluids attenuates the outgoing mode of S0 mode, where attenuation of the

mode $\mathrm{Im}(\xi_{zm})$ is positive. While the incoming mode is amplified as it propagates due to an inflow of wave energy from the external fluids, namely $\mathrm{Im}(\xi_{zm})$ is negative.

The A0 mode also has outgoing and incoming modes at the same point B on the dispersion curve of Fig. 2 (a), as shown in Fig. 4. Unlike the fundamental Lamb modes, Scholte waves have two wave structures without propagating in the *y* direction, which results from the wavenumber with $\mathrm{Re}(\xi_{ym}) = 0$. As shown in Figs. 5 (a) and (b), the Scholte waves forms symmetric and anti-symmetric distributions with respect to the center line of plate thickness. Because the symmetric and anti-symmetric modes have identical phase and group velocities each other beyond the *fd* value of about 1 MHz mm, modes obtained by taking their summation and difference can also be considered as the wave structures at this point. Figures 5 (c) and (d) show that the summation and difference of the symmetric and anti-symmetric modes gives the modes vibrating only at a single fluid region and a plate surface.

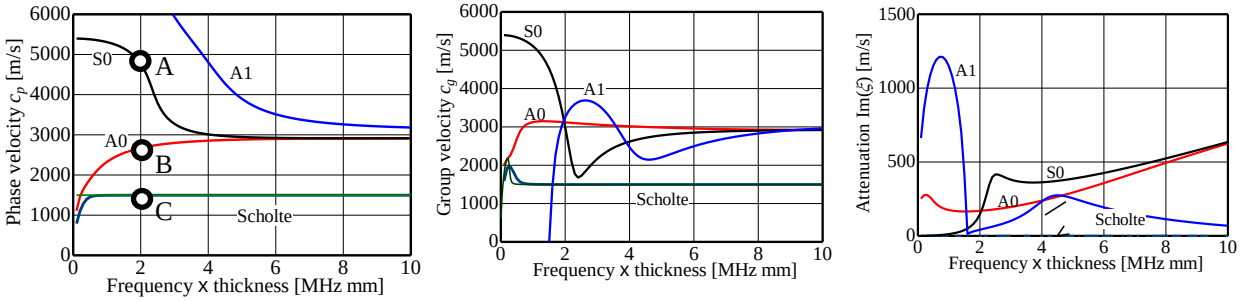

(a) Phase velocity (b) Group velocity (c) Attenuation

FIGURE 2. Dispersion curves for leaky plate modes in an aluminum plate surrounded by water

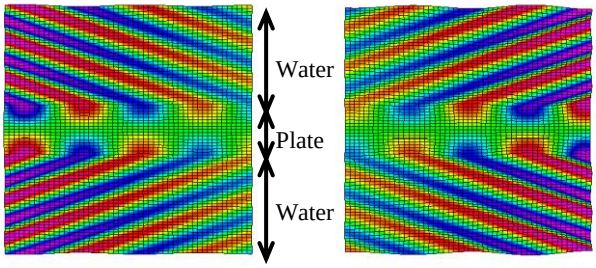

(a) Outgoing mode (b) Incoming mode

FIGURE 3. Wave structures for a point A in Fig. 2 (a).

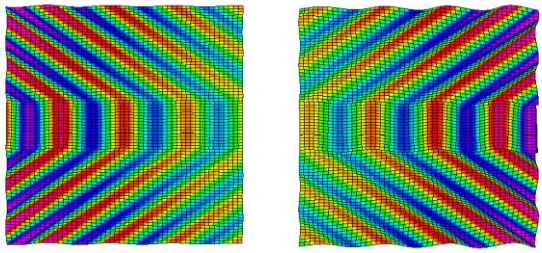

(a) Outgoing mode (b) Incoming mode

FIGURE 4. Wave structures for a point B in Fig. 2 (a).

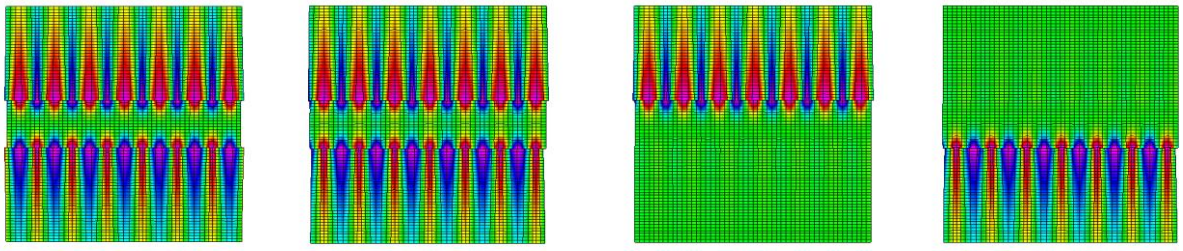

(a) Symmetric Scholte wave (b) Anyi-symmetric Scholte wave (a) Summation of (a) and (b) (b) Difference of (a) and (b)

FIGURE 5. Wave structures at a point C in Fig. 2 (c) for Scholte waves

Dispersion Curves and Wave Structures of Total Transmission Modes

When solving eigenvalue problem of eq. (9) using the second equation of eq. (6), dispersion curves for total transmission modes are obtained. As in leaky plate modes, we can find several differences in dispersion curves from a plate with no leaky media which include existence of Scholte wave, attenuation of S0 and A0 modes, and non-smoothness of the A0 mode in low *fd* range. In addition, the A0 mode and the S0 mode merge perfectly beyond the *fd* value of about 3.5 MHz mm and group velocity is significantly changed and attenuation suddenly appears at the *fd* value.

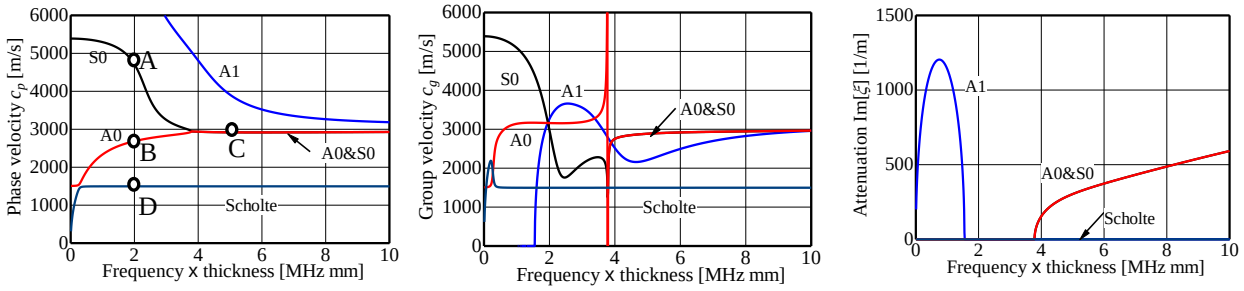

(a) Phase velocity (b) Group velocity (c) Attenuation

FIGURE 6. Dispersion curves for total transmission modes in an aluminum plate surrounded by water

Figures 7, 8, 9, and 10 are wavestructures for the points A, B, C, and D in Fig. 6 (a), respectively. Like in leaky plate modes, two different wave structures corresponding to a pair of $\pm\xi_{ym}$ exist as shown in Fig. 7 and 8, one being an upward total transmission mode, and the other one being a downward mode. While four wave structures exist beyond the *fd* value at which A0 and S0 modes merge as shown in Fig. 9 for the point C. They are outgoing and incoming modes vibrating in a single fluid region and their vertically inverted images. As in leaky plate modes, outgoing modes having positive Im(ξ_{zm}) attenuate as they propagate due to energy leakage, while incoming modes having negative Im(ξ_{zm}) increase their amplitude as they propagate.

Scholte waves in Fig. 6 (a) have pure imaginary wave numbers of ξ_{ym} like in the case of leaky plate modes, which means that vibration in one fluid region exponentially decay and vibration in the other fluid region exponentially increase according to the distance from plate surfaces in the case of total transmission. However, at the point D, Scholte wave exists only at the other fluid region as seen in Fig. 10 because displacement in the *y* direction are zero at the surface contacting with the fluid region where the amplitude exponentially increase as going further from it, which results in the same mode as the Scholte wavs obtained in Fig. 5 (c) and (d).

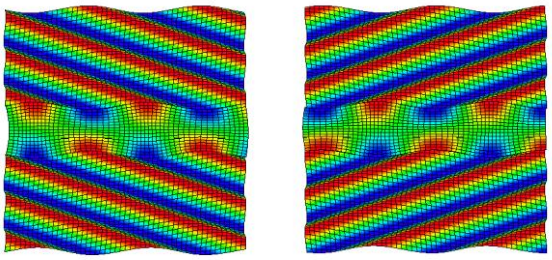

(a) Upward mode (b) Downward mode

FIGURE 7. Wave structures for a point A in Fig. 6 (a).

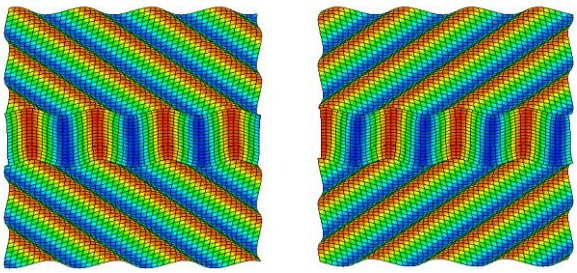

(a) Upward mode (b) Downward mode

FIGURE 8. Wave structures for a point B in Fig. 6 (a).

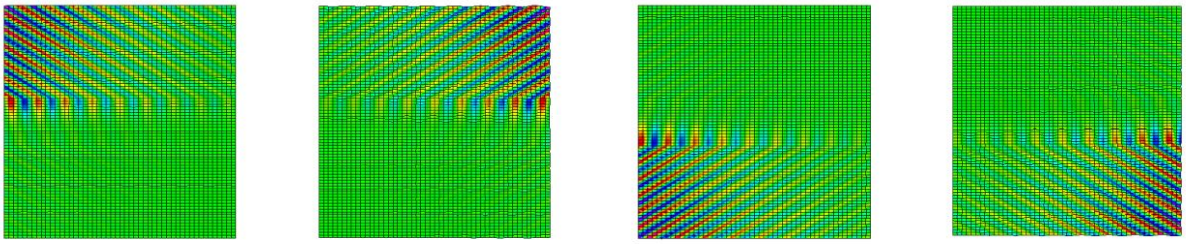

(a) Outgoing mode vibrating only at an upper region (b) Incoming mode vibrating only at an upper region (c) Outgoing mode vibrating only at a lower region (d) Incoming mode vibrating only at a lower region

FIGURE 9. Wave structures at a point C in Fig. 6 (a)

(a) Scholte wave propagating along the lower surface (b) Scholte wave propagating along the upper surface

FIGURE 10. Wave structures at a point D in Fig. 6 (a)

Scholte Waves in a Low *fd* Range

Scholte waves obtained from both leaky plate modes and total transmission modes are non-dispersive with the identical phase velocities and group velocities in the high *fd* range, which results from the nature that the Scholte waves are modes with the same wave structures vibrating at a single plate – fluid interface as seen in Fig. 5 (c), (d) and Fig. 10 (a), (b).

However, looking at the dispersion curves in the low *fd* range below about 1 MHz mm, Scholte waves have differences between leaky plate mode and total transmission mode. Figure 11 is phase velocity dispersion curves in the low *fd* range below 2 MHz mm. In the leaky plate mode in Fig. 11 (a), anti-symmetric and symmetric Scholte waves separate apart at about *fd* = 0.7 MHz mm, and an anti-symmetric Scholte wave goes to origin of the graph while a symmetric Scholte wave keeps straight with the constant velocity. Figures 12 (a) and (b) are wave structures of Scholte waves at the two points A and B on *fd* = 0.2 MHz mm obtained from leaky plate modes. The anti-symmetric Scholte wave at the point A shown in Fig. 12 (a) vibrates whole thickness of a plate mainly in the thickness direction as well as the fluid regions close to the plate – fluid interface. Figures 10 and 12 (a) represent that energy of vibration concentrates at a single side of plate surfaces in the high *fd* range, while it penetrates deeper as an *fd* value becomes lower and a whole cross-section of a plate vibrates at the point of A in Fig. 11 (a). Therefore, the dispersion curve is dependent on the *fd* value. While, in the symmetric mode Fig. 12 (b) at the point B, vibration in the thickness direction concentrates only at the both plate surfaces. Since this mode vibrates horizontally in fluid regions as a plane longitudinal wave, the non-dispersive mode has almost the same velocity as sound speed of the fluid (water).

For comparison, Fig. 12 (c) shows a wave structure of an A0 mode at the point C in Fig. 11. Although the A0 mode is similar to the mode in Fig. 12 (a) in terms of vibrating a whole cross-section in the thickness direction, the mode propagates in very short distance due to its high attenuation.

Scholte waves obtained as total transmission modes also exist two modes with different wave structures, but these two modes have the identical phase velocities over the whole *fd* range. Figures. 13 (a) and (b) show the two wave structures of Scholte waves at the point D in Fig. 11 (b). Although Scholte waves obtained as total transmission modes in Fig. 10 vibrate only a single side of plate surfaces in the high *fd* range, displacement distributions at the plate surface penetrate deeper as *fd* range become lower, resulting in vibration at the opposite

surface in the *fd* range at the point D and the exponentially increasing displacement distribution in the opposite fluid region.

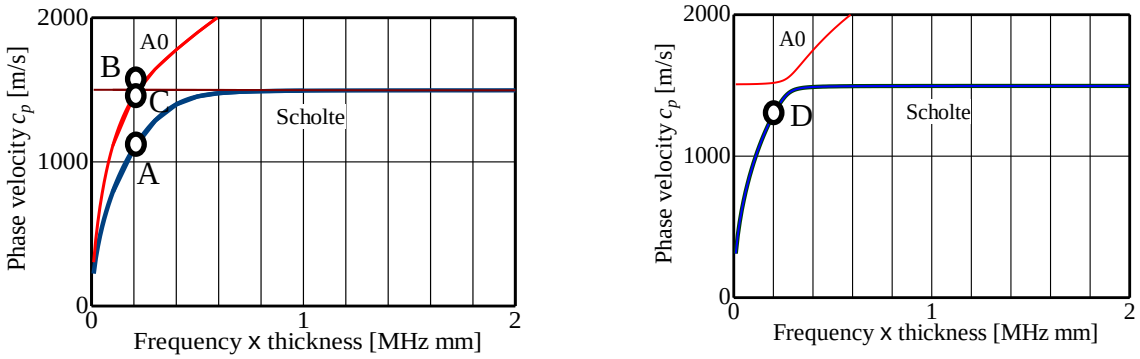

(a) Leaky plate modes (b) Total transmission modes

FIGURE 11. Low fd range of phase velocity dispersion curves

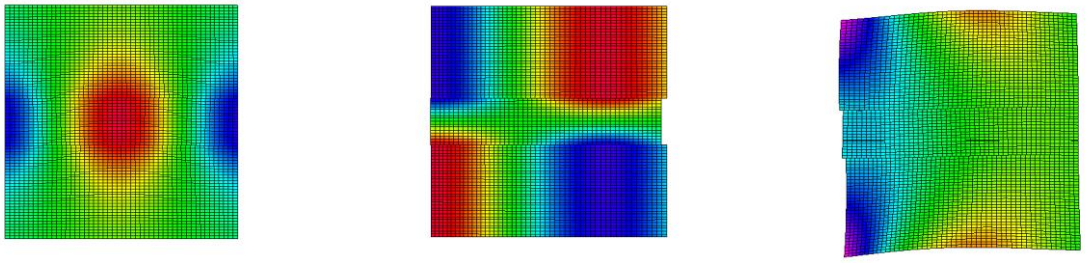

(a) point A. Anti-symmetric Scholte wave. (b) point B Symmetric Scholte wave. (c) point C. A0 mode

FIGURE 12. Wave structures for points A-C in Fig. 11(a) obtained as leaky Lamb waves

(a) Exponentially increasing displacement distribution in the upper fluid region (b) Exponentially increasing displacement distribution in the lower fluid region

FIGURE 13. Wave structures for a point D in Fig. 11(b) obtained as total transmission waves

CONCLUSIONS

This paper described the formulation of a SAFE method for Lamb waves in a plate with leaky media by comparing with a SAFE for a plate with no leaky media, and then fundamental modes of Lamb waves and Scholte waves were analyzed with their dispersion curves and wave structures.

Solutions are classified into leaky plate modes and total transmission modes by the way how positive directions of plane harmonic wave in fluids are assigned. Their phase velocity dispersion curves and ones with no leaky media are slightly different each other. In particular, dispersion curves for S0 and A0 modes are identical beyond a certain *fd* value in total transmission modes and four different modes with symmetric wave structures exist in the high *fd* range.

Scholte waves obtained as leaky plate modes consist of two modes with the same phase velocity, group velocity and attenuation in the high *fd* range over *fd* = 1 MHz mm showing anti-symmetric and symmetric wave structures with respect to the plate center. Taking summation or difference of these two wave structures, these modes can be regarded as a Scholte wave propagating only at a single side of plate surfaces. Scholte wave obtained as total transmission modes also consist of two modes with different wave structures. In the high *fd* range over 1 MHz mm, these modes have the identical dispersion curves and wave structures vibrating only at a single plate surface.

In the low *fd* range below about 1MHz mm, dispersion curves of Scholte waves are significantly different in these two cases, which results in the fact that vibration at a plate surface affects the opposite surface due to low *fd* value.

ACKNOWLEDGMENTS

This work was supported by JSPS KAKENHI Grant Number 26282094. The author would like to thank Professor Shiro Biwa for his continuing encouragement.

REFERENCES

1. Y. K. Cheung, J. of Eng. Mech. Div., Proc. of ASCE **94**, 1365 -1378 (1968).
2. R.B. Dong, S. B., Nelson, J. Appl. Mech. **39**, 739 - 745 (1972).
3. R.L. Datta, S. K., Shah A. H., Bratton and T. Chakraborty, J. Acoust. Soc. Am. **83**, 2020 - 2026 (1988).
4. E. Kausel, Int. J. Numer. Methods Eng. **23**, 1567 - 1578 (1986).
5. L. Gavrić, J. S Sound Vib. **185**, 531 - 543 (1995).
6. L. Gray, J. Sound Vib. **195**, 477 - 505 (1996).
7. D.J. Thompson and C.J.C. Jones, J. Sound Vib. **253**, 401 - 409 (2002).
8. P.W. Loveday, IEEE Trans. Ultrason. Ferroelectr. Freq. Control **55**, 2038 - 2045 (2008).
9. M. Castaings and M. Lowe, J. Acoust. Soc. Am. **123**, 696 - 708 (2008).
10. M. Mazzotti, a. Marzani, I. Bartoli, and E. Viola, Int. J. Solids Struct. **49**, 2359 - 2372 (2012).
11. T. Hayashi, W.-J. Song, and J.L. Rose, Ultrasonics **41**, 175 - 183 (2003).
12. M. Mazzotti, I. Bartoli, A. Marzani, and E. Viola, Ultrasonics **53**, 1227 - 1241 (2013).
13. T. Hayashi and D. Inoue, Ultrasonics **54**, 1460 - 1469 (2014).
14. D.E. Chimenti and S.I. Rokhlin, J. Acoust. Soc. Am. **88**, 1603 - 1611 (1990).